Equation (2) is not valid when $\dot{y}_0 = 0$, i.e., for the rectilinear cases. Substituting (5), however, into (1) and (2),

$$x\dot{g} - g\dot{x} = r_0 \tag{6}$$

$$x\dot{x} + bg\dot{g} = \dot{r}_0 x + cg \tag{7}$$

$$b = \dot{y}_0^2 = v_0^2 - \dot{r}_0^2 \qquad c = b - \mu/r_0 \qquad v_0 = |\dot{\mathbf{r}}_0|$$

$$x_0 = r_0 \qquad g_0 = 0 \tag{8}$$

Substitution of

$$x = \sum_{i=0}^{\infty} a_i(t - t_0)^i \qquad g = \sum_{i=0}^{\infty} b_i(t - t_0)^i \tag{9}$$

into (6) and (7) with $a_0 = r_0$, $a_1 = \dot{r}_0$, $b_0 = 0$, and $b_1 = 1$ gives, for $i \geq 1$,

$$r_0(i + 1)a_{i+1} = a_1 a_i + cb_i - \sum_{j=0}^{i-1} (j + 1)(a_{j+1}a_{i-j} + bb_{j+1}b_{i-j}) \tag{10}$$

$$r_0(i + 1)b_{i+1} = \sum_{j=0}^{i-1} (j + 1)(a_{j+1}b_{i-j} - b_{j+1}a_{i-j}) \tag{11}$$

Taking advantage of symmetry in the summations, (10) and (11) become, for $i \geq 2$,

$$r_0 a_{i+1} = \frac{(a_1 a_i + cb_i)}{(i + 1)} - \sum_{j=0}^{k} a_{j+1}a_{i-j} - b\sum_{j=0}^{k} b_{j+1}b_{i-j} - q(a_{k+2}^2 + bb_{k+2}^2) \tag{12}$$

$$r_0(i + 1)b_{i+1} = \sum_{j=0}^{k} [(i - j) - (j + 1)] \times (b_{j+1}a_{i-j} - a_{j+1}b_{i-j}) \tag{13}$$

k = integral part of $\frac{1}{2}(i - 2)$

q = fractional part of $\frac{1}{2}(i - 2)$

$a_2 = -\mu/2r_0^2 \qquad b_2 = 0$

Having $x(t)$ and $g(t)$, f can be computed from (4) and $\mathbf{r}(t)$ from (3). Inversion of (6) and (7) yields

$$r^2\dot{x} = (\dot{r}_0 x + cg)x - br_0 g \tag{14}$$

$$r^2\dot{g} = r_0 x + (\dot{r}_0 x + cg)g \tag{15}$$

where

$$r^2 = x^2 + bg^2$$

Then $\dot{f}(t)$ and $\dot{\mathbf{r}}(t)$ are obtained from

$$\dot{f} = (\dot{x} - \dot{r}_0 g)/r_0 \qquad \dot{\mathbf{r}} = f\dot{\mathbf{r}}_0 + g\ddot{\mathbf{r}}_0$$

For purposes of numerical control it may be advisable to let

$$t - t_0 = h\tau \qquad h = t_1 - t_0$$

where $[t_0, t_1]$ is a time interval of interest. The corresponding interval for τ is [0, 1]. Equations (12) and (13) still hold provided $a_0 = r_0$, $b_0 = b_2 = 0$, $a_1 = \dot{r}_0 h$, $b_1 = h$, $a_2 = -\mu h^2/2r_0^2$, $c = (b - \mu/r_0)h$. Equations (9) become

$$x = \sum_{i=0}^{\infty} a_i\tau^i \qquad g = \sum_{i=0}^{\infty} b_i\tau^i$$

which offer a further advantage when $t = t_1$, i.e., when $\tau = 1$. Formulas for the radii of convergence of the f and g series are given by Moulton.[1]

Reference

[1] Moulton, F. R., "The True Radii of Convergence of the Expressions for the Ratios of the Triangles When Developed as Power Series in the Time Intervals," *The Astronomical Journal*, Vol. 23, 1903, pp. 93–102.

Vehicle Mass-Exhaust Velocity Variations in Free Space

Louis G. Vargo*
Western New Mexico University, Silver City, N. Mex.

Nomenclature

p	=	unexpected mass exclusive of payload (initial total vehicle mass = 1)
l	=	payload mass
$e(t)$	=	onboard expellant mass (initial expellant mass = e_0)
$\tilde{e}_0$	=	optimum initial expellant mass
α, β, γ	=	thrust, expellant, and power coefficients, respectively
$c(t)$	=	effective exhaust velocity
T	=	total propulsion time
v	=	required mission velocity

In a previous paper[1] the writer and two associates presented a generalized analysis of space vehicle performance in which the unexpended mass of the vehicle exclusive of the payload includes three mass fractions: a fraction proportional to the initial mass of expellant and fractions proportional to the average thrust and power output of the propulsion system. "Thrust-limited" and "power-limited" classes of vehicles were thus combined in a single representation. The analytical method used was a straightforward application of the Euler condition in seeking a payload maximum subject to the mission velocity requirement. It was shown that the payload expression,

$$l = 1 - p - e_0 = 1 - \int_0^T \left[(1 + \beta)\dot{e} + \frac{\alpha}{T}\dot{e}c + \frac{\gamma}{2T}\dot{e}c^2\right] dt = 1 - \int_{e_0}^{0} \left[1 + \beta + \frac{\alpha}{T}c(e) + \frac{\gamma}{2T}c^2(e)\right] de \tag{1}$$

is extremized when mass-exhaust velocity variations follow

$$\frac{c(e)}{v} = -\frac{\alpha}{\gamma v} + \frac{(1 - e_0)}{e_0(1 - e_0 + e)}\left[1 - \frac{\alpha}{\gamma v}\ln(1 - e_0)\right] \tag{2}$$

for *any* e_0 and is further maximized when the vehicle is designed for an initial expellant mass satisfying the transcendental equation,

$$\left\{1 - \frac{\alpha}{\gamma v}[\tilde{e}_0 + \ln(1 - \tilde{e}_0)]\right\}^2 = \frac{2(1 + \beta)T\tilde{e}_0^2}{\gamma v^2} \tag{3}$$

The purpose of the present Note is to publicize the results of the original paper in a wider forum and to investigate the last two equations more closely. Equation (2) is of the form

$$(e_0/v)ec - k_1 e + k_2 c + k_3 = 0 \tag{4}$$

and, since the discriminant $(e_0/v)^2$ of this conic is always positive, e and c vary optimally along an hyperbola. Now e monotonically decreases (at least piecewise) with time. Thus c must either decrease or increase piecewise monotonically since the asymptotes of Eq. (4) are parallel with the coordinate axes. These asymptotes are the lines $c = -\alpha/\gamma$, $e = -(1 - e_0)$ below and to the left of the axes. Therefore, we have shown that an optimal exhaust velocity program increases during the powered phases of the mission, regardless of the initial expellant loading, and depends numerically only on the nondimensional vehicle-mission parameter $\alpha/\gamma v = D$ and the initial expellant fraction. The normalized exhaust velocity c/v has a relative variation of

$$\frac{e_0[1 - D\ln(1 - e_0)]}{(1 - e_0)[1 - D\ln(1 - e_0)] - e_0 D}$$

Received June 7, 1967.

*Instructor, Department of Mathematics.

For the case of negligible thrust dependency $\alpha \approx 0$ or for very ambitious missions $v \gg \alpha/\gamma$, this relative variation approaches $e_0/(1 - e_0)$, the ratio of expellant to nonexpellant mass. For negligible power dependency $\gamma \approx 0$ or very modest missions $v \ll \alpha/\gamma$, no such simple limit exists.

It may be shown further that designs at optimum expellant loading have a final normalized exhaust velocity value which is a function of only the other nondimensional parameter $(1 + \beta)T/\gamma v^2 = E$. Solving Eq. (3) for $ln(1 + \tilde{e}_0)$ and substituting into Eq. (2) yields

$$\frac{c}{v} = \frac{(2E)^{1/2}(1 - \tilde{e}_0) - De}{(1 - \tilde{e}_0) + e} \tag{5}$$

At $t = 0$, $e = \tilde{e}_0$ and $c(0)/v = (2E)^{1/2}(1 - \tilde{e}_0) - D\tilde{e}_0$. At $t = T$, $e = 0$ and $c(T)/v = (2E)^{1/2}$ The last equation can be regarded as a fundamental design relationship for space propulsion systems. On rewriting it becomes $\gamma c_{max}{}^2 = 2(1 + \beta)T$ and in this form allows hardware preliminary design alternatives to be compared easily with respect to their ultimate system utility.

Reference

[1] Vargo, L. G., DeLong, G. W., and DeBilzan, C. C., "The Hybrid Space Vehicle and Its Performance," *Proceedings of the Fifth International Symposium on Space Technology and Science*, Sept. 1963, Tokyo, Japan.

Friction and Heat Transfer in the Flow Induced by a Subsonic Heat Source

JOHN H. SKINNER JR.*
Rensselaer Polytechnic Institute, Troy, N. Y.

Introduction

THIS Note presents the second part of a study[2,3] of the effects of friction and heat transfer on the flowfield induced by a disturbance traveling at a constant velocity through an infinite tube.

In order to study the flow induced by a disturbance traveling subsonically at a constant velocity, the following model is considered. One half of an infinite tube is filled with a combustible mixture, and the other half is filled with an inert gas. The gas is initially in uniform state and at rest everywhere with the tube. A constant-velocity subsonic heat source is produced using a steady burning fuse, or by firing a series of spark plugs in succession along the tube walls. On ignition, a forward-facing shock starts traveling through the mixture while a rearward-facing shock starts propagating through the inert gas (Fig. 1). An interface between burned and inert gas also travels through the duct. The following assumptions are made:

1) The heat source is a one-dimensional discontinuity across which the flow is quasi-steady.

2) The time rate of heat release of the heat source is constant. Because of the forward-facing shock, the gas ahead of the heat source is in motion. Dissipative effects will alter this motion, and the mass rate of flow and heat release per unit mass across the heat source will be time-dependent. The product of these two parameters is, however, invariant with respect to time, by virtue of the present assumption.

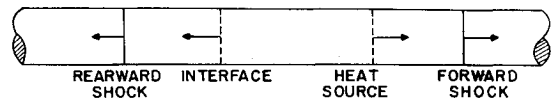

Fig. 1 Situation after ignition.

3) The flow is one-dimensional, fully developed, and turbulent in the entire flowfield between the forward- and rearward-facing shocks.

4) The gases are ideal, and the ratio of specific heats is constant.

This model is analyzed by the method of characteristics for one-dimensional nonsteady flow[4] with inclusion of friction and heat-transfer effects.

The characteristic equations are integrated numerically for the specific case of a heat source traveling at a nondimensional velocity of $U_D = 0.5$ and with a nondimensional time rate of heat release of $\dot{J} = 3.19$, and for the following conditions (same notation as in Ref. 3): $C_f = 0.01$, $r = 2$ in., $\gamma = 1.4$, and $L_0 = 5.280$ ft.

Discussion of Results

If the flow is assumed inviscid and adiabatic, the resulting flowfield is uniform in the region between the forward-facing shock and the heat source and then again in the region between the heat source and the interface. Therefore, in these regions, the flow is steady in a frame of reference moving with the heat source. It is interesting to compare this phenomenon with its counterpart in the supersonic case, where, because of an expansion wave behind the detonation, the inviscid adiabatic flowfield is nonsteady in the detonation-fixed coordinate system.

Figure 2 shows the velocity distribution in the wake region, in a coordinate system moving with the heat source, for flow with friction and heat transfer. In this figure, τ is nondimensionalized time, whereas ξ is the nondimensional distance from the heat source.

Since for very short initial time intervals the integrated effects of friction and heat transfer are small, the initial flowfield is substantially that predicted by inviscid adiabatic analysis. Figure 2 shows that, as time progresses, friction and heat transfer cause a timewise variation of the flowfield, and the flow becomes nonsteady. This is the direct opposite of the supersonic case, where the initially nonsteady flowfield was modified to one that was steady in the frame of reference moving with the detonation.

Since the detonation travels at supersonic velocity relative to the wake region, signals traveling at sonic speed can never

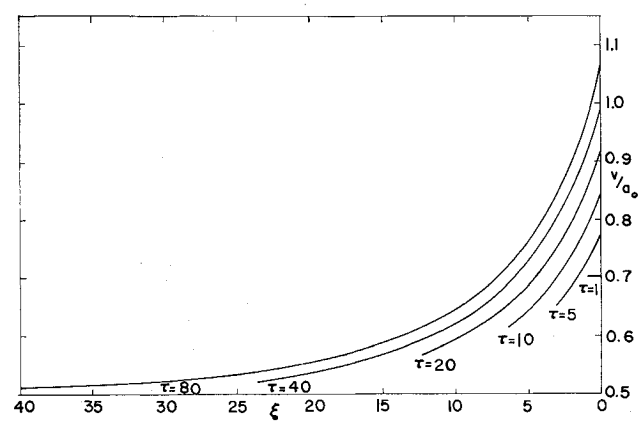

Fig. 2 Velocity distribution in the wake region in a coordinate system fixed to the heat source.

Received September 20, 1967; revision received November 27, 1967. This paper is taken from part of a thesis to be submitted in partial fulfillment of the requirements for the degree of Doctor of Philosophy in the Department of Aeronautical Engineering and Astronautics at Rensselaer Polytechnic Institute. This research was supported in part by a NASA Traineeship and in part by the U.S. Department of Transportation under Contract C-117-66 (Neg.) and is reported in detail in Ref. 1.

* Graduate Student, Department of Aeronautical Engineering and Astronautics.